Molecular Immunology 154 (2023) 33–44

Contents lists available at ScienceDirect

Molecular Immunology

journal homepage: www.elsevier.com/locate/molimm

A subset of leukocyte immune-type receptors (LITRs) regulates phagocytosis in channel catfish (*Ictalurus punctatus*) leukocytes

Jonathan Crider[a,b], Melanie Wilson[a,b], Kristianna L. Felch[a,b], Rebecca A. Dupre[c,d], Sylvie M.A. Quiniou[e], Eva Bengtén[a,b,*]

[a] *Center for Immunology and Microbial Research, University of Mississippi Medical Center, 2500 North State Street, Jackson, MS 39216, USA*
[b] *Department of Cell and Molecular Biology, University of Mississippi Medical Center, 2500 North State Street, Jackson, MS 39216, USA*
[c] *Oak Ridge Institute for Science and Education, US Department of Energy, 1299 Bethel Valley Rd, Oak Ridge, TN 37831-0117, USA*
[d] *Food Processing and Sensory Quality Unit, USDA-ARS, 1100 Allen Toussaint Blvd, New Orleans, LA 70124, USA*
[e] *Warmwater Aquaculture Research Unit, USDA-ARS-WARU, P.O. BOX 38, Stoneville, MS 38776, USA*

ARTICLE INFO

Keywords:
Paired receptors
Immunoregulatory receptors
Phagocytosis
Inhibitory signaling
Cytoplasmic tails
Innate immunity
Leukocyte immune-type receptors
Channel catfish

ABSTRACT

Channel catfish, *Ictalurus punctatus,* leukocyte immune-type receptors (LITRs) constitute a large family of paired, immunoregulatory receptors unique to teleosts. A role for LITRs in phagocytosis has been proposed based on studies in mammalian cell lines; however, LITR-mediated phagocytosis has not been examined in the catfish model. In this study, we use two anti-LITR monoclonal antibodies, CC41 and 125.2, to contrast the effects of crosslinking subsets of inhibitory and activating LITRs. Briefly, LITRs expressed by catfish γδ T cells, αβ T cells, and macrophage cell lines were crosslinked using mAb-conjugated fluorescent microbeads, and bead uptake was evaluated by flow cytometry and confirmed by confocal microscopy. A clear difference in the uptake of 125.2- and CC41-conjugated beads was observed. Crosslinking LITRs with mAb 125.2 resulted in efficient bead internalization, while mAb CC41 crosslinking of inhibitory LITRs resulted predominantly in a capturing phenotype. Pretreating catfish macrophages with mAb CC41 resulted in a marked decrease in LITR-mediated phagocytosis of 125.2-conjugated beads. Overall, these findings provide insight into fish immunobiology and validate LITRs as regulators of phagocytosis in catfish macrophages and γδ T cells.

1. Introduction

Paired receptors are families of membrane-bound inhibitory or activating receptors that regulate essential innate immune functions such as cell-mediated cytotoxicity, degranulation, and phagocytosis. Multiple families of paired receptors have been identified in vertebrates (Kuroki et al., 2012; Schwarz et al., 2017; Borrego, 2013; Barclay and van den Berg, 2014). Their ligand-binding extracellular domain structures place them either into the immunoglobulin superfamily (IgSF; e.g., FcRs, FCRLs, KIRs, LILRs, SIRPs, CD200R, CD300, TREMs, CEACAMs) or

---

Abbreviations: APC, Allophycocyanin; μME, μMercaptoethanol; BSA, Bovine Serum Albumin; cfPBS, Catfish Tonicity Phosphate Buffered Saline; cfRPMI, Catfish Tonicity RPMI 1640; CCV, Channel Catfish Virus; CEACAM, Carcinoembryonic Antigen-Related Cell Adhesion Molecules; Csk, C-terminal Src Kinase; CTL, Cytotoxic T Lymphocytes; CYT, Cytoplasmic Tail; DAP10, DNAX-Activating Protein of 10 kDa; DAP12, DNAX-Activating Protein of 12 kDa; DICP, Diverse Immunoglobulin (Ig) Domain-Containing Protein; FcR, Fc Receptor; FcRL, Fc Receptor-Like; HA, Hemagglutinin; Ig, Immunoglobulin; IgSF, Immunoglobulin Super Family; ITAM, Immunoreceptor Tyrosine-based Activation Motif; ITIM, Immunoreceptor Tyrosine-based Inhibition Motif; ITSM, Immunoreceptor Tyrosine-based Switch Motif; KIR, Killer Cell Immunoglobulin-Like Receptors; LAK, Lymphokine-Activated Killer; LILR, Leukocyte Immunoglobulin-Like Receptors; LITR, Leukocyte Immune-Type Receptor; MHC, Major Histocompatibility Complex; MLC, Mixed Leukocyte Culture; nanoLC-MS/MS, Nanoscale Liquid Chromatography Coupled to Tandem Mass Spectrometry; Nck, Non-catalytic region of tyrosine kinase; NILT, Novel Immunoglobulin-Like Transcript; NITR, Novel Immune-Type Receptor; NK, Natural Killer; NKG2D, Natural Killer Group 2D; PBL, Peripheral Blood Leukocytes; PIGRL, Polymeric Immunoglobulin Receptor; RBL, Rat Basophilic Leukemia; TM, Transmembrane; TREM, Triggering Receptors Expressed on Myeloid cells; SHP-2, Src Homology-2 Domain-Containing Protein Tyrosine Phosphatases – 2; Siglec, Sialic-Acid-Binding Immunoglobulin-Like Lectins; SIRP, Signal-Regulatory-Protein; WGA, Wheat Germ Agglutinin.

[*] Corresponding author at: Center for Immunology and Microbial Research, University of Mississippi Medical Center, 2500 North State Street, Jackson, MS 39216, USA.

E-mail addresses: jcrider@umc.edu (J. Crider), mwilson@umc.edu (M. Wilson), ksaelens@umc.edu (K.L. Felch), rebecca.dupre@usda.gov (R.A. Dupre), sylvie.quiniou@usda.gov (S.M.A. Quiniou), ebengten@umc.edu (E. Bengtén).

https://doi.org/10.1016/j.molimm.2022.12.009
Received 30 September 2022; Received in revised form 12 December 2022; Accepted 15 December 2022

into the C-type lectin-like family (e.g., Ly49, NKG2D, CD94-NKG2, Siglecs; reviewed in Akkaya and Barclay, 2013; Martinet and Smyth, 2015). While inhibitory and activating paired receptors display a high percentage of amino acid sequence identity in their extracellular domains, their transmembrane and cytoplasmic regions differ (Yamada and McVicar, 2008). Inhibitory receptors have a neutral transmembrane (TM) region, a long cytoplasmic tail (CYT) with one or more inhibitory motifs, i.e., immunoreceptor tyrosine-based inhibitory motifs (ITIMs) and immunoreceptor tyrosine-based switch motifs (ITSMs; reviewed in Billadeau and Leibson, 2002; Daëron et al., 2008). In contrast, activating paired receptors usually have a shorter CYT and a charged residue (lysine or arginine) in their TM region, which mediates their association with signaling adaptor molecules, such as the DAP10, DAP12, or the FcRγ signaling chain (Vély and Vivier, 1997; reviewed in Lanier, 2009).

In teleosts, unique families of IgSF paired immunoregulatory receptors include novel immune-type receptors (NITRs; Strong et al., 1999; Yoder et al., 2001, 2004; Evenhuis et al., 2007; Wei et al., 2007; Dornburg et al., 2021); polymeric immunoglobulin receptor-like proteins (PIGRL; Ribeiro et al., 2011; Kortum et al., 2014; Etayo et al., 2022); diverse immunoglobulin domain-containing proteins (DICPs; Haire et al., 2012; Boudinot et al., 2014; Rodriguez-Nunez et al., 2016; Gao et al., 2018); novel immunoglobulin-like transcripts (NILTs; Stet et al., 2005; Kock and Fischer, 2008; Østergaard et al., 2009, 2010; Rodríguez-Nunez et al., 2014; Wcisel et al., 2022), and leukocyte immune-type receptors (LITRs; Stafford et al., 2006; Stafford et al., 2007; Wang et al., 2020). Leukocyte immune-type receptors were first identified in channel catfish, and they constitute a large, diverse receptor family expressed by catfish NK cells, cytotoxic T cells, B cells, and 42TA macrophages (Stafford et al., 2006). Our initial phylogenetic analyses of IpLITR Ig domains suggested that LITRs shared a common ancestor with FCRs and FCRLs. This evolutionary relationship was supported by recent genomic analyses and comparisons of genomes from teleosts and other vertebrates (Wang et al., 2021). Moreover, this review demonstrated conserved synteny between LITR and FCRL chromosomal regions, i.e., teleost LITRs, like FCRLs in *Xenopus tropicalis* and humans, are encoded on large genomic clusters that are linked to genes encoding slam family members, vangl2, and arhgedf11 (Wang et al., 2021).

Functional studies using epitope-tagged, chimeric LITRs overexpressed in heterologous systems have yielded valuable insights into LITR signaling and its potential roles in degranulation and phagocytosis (Fei et al., 2016). For example, in transient transfections of human embryonic kidney (HEK) 293 T cells, activating IpLITR2.6b associated with epitope-tagged IpFcRγ, IpFcRγ-L, or IpCD3ζ-L adaptor proteins (Mewes et al., 2009). Building on this work, Montgomery et al., 2009, 2012, expressed chimeric receptors consisting of the human KIR2DL3 fused with the CYT regions of inhibitory IpLITR1.1b or IpLITR1.2a in mouse lymphokine-activated killer (LAK) cells using a vaccinia virus vector. This model demonstrated that IpLITR CYTs could inhibit the killing of B cells that expressed the KIR2DL3 ligand, HLA-Cw3, on their surface (Montgomery et al., 2012). Importantly, Src homology-2 domain-containing protein tyrosine phosphatases (SHP)- 1, SHP-2, and C-terminal Src kinase (Csk) were shown to participate in the inhibitory signaling activity of ITIM-containing IpLITR1.1b following phosphorylation (Montgomery et al., 2009, 2012). In a complementary study, Cortes et al. (2012), stably expressed hemagglutinin (HA)-tagged IpLITR2.6b-FcRγ-L chimeric receptors in rat basophilic leukemia (RBL-2H3) cells, and crosslinking these tagged receptors activated the Erk1/Erk2 pathway and induced degranulation. Furthermore, the HA-tagged IpLITR chimeric receptors mediated phagocytosis of anti-HA opsonized microbeads. More recently, imaging flow cytometry and confocal microscopy demonstrated that activating IpLITR2.6b-FcRγ-L and inhibitory IpLITR1.1b mediate signaling events that result in F-actin polymerization and the formation of phagocytic cups (Zwozdesky et al., 2017; Lillico et al., 2018, 2020; Jones and Stafford, 2019). However, only the activating IpLITR2.6b mediated efficient bead uptake and phagosome formation. This uptake was accompanied by an accumulation of phosphotyrosines within the phagocytic cups. The simultaneous cross-linking of the activating IpLITR2.6b and the inhibitory IpLITR1.1b resulted in 50 % reduced phosphotyrosine activity compared to cross-linking IpLITR2.6b alone (Fei et al., 2020). These studies confirmed that IpLITR 1.1b is an effective inhibitor of IpLITR2.6b/IpFcRγ-L-mediated phagocytosis in mammalian cells. However, IpLITR-mediated phagocytosis has not been examined in the catfish model.

One of the strengths of the channel catfish model is its viable in vitro cell culture system and the long-term functionally distinct clonal lymphocyte and macrophage cell lines (Miller et al., 1987; Vallejo et al., 1991; Miller et al., 1994a, 1994b, 1998; Clem et al., 1996; Stuge et al., 1997; Taylor et al., 2020). The catfish long-term B, T, and macrophage cell lines were established without using transformation protocols, while our NK and cytotoxic T lymphocytes (CTL) lines were developed using allogeneic stimulation (Shen et al., 2002, 2003, 2004; Stuge et al., 2000). Two of these cell lines, NK TS10.1 and CTL TS32.15, were used separately to immunize Balb/c mice and develop monoclonal antibodies. One mAb, CC41, reacted with subsets of long LITR isoforms expressed at high density on catfish cytotoxic T cells and NK cells (Shen et al., 2004; Taylor et al., 2016). Importantly, we demonstrated that CC41 could be used to monitor in vivo cytotoxic cell responses to infection with channel catfish virus (CCV). An increase in the population of CC41$^{\text{bright}}$ peripheral blood leukocytes (PBLs) was readily observed five days after immunization (Taylor et al., 2016). These CC41$^{\text{bright}}$ PBLs specifically killed CCV-infected syngeneic targets. Notably, pre-treatment of cytotoxic cells with mAb CC41 resulted in a 40 % reduction in their cytotoxic activity against CCV-infected targets, and based on this inhibition, we hypothesized that mAb CC41 preferentially binds inhibitory IpLITR isoforms. In a follow-up study, Blackmon et al., 2020, developed a co-culture model using catfish head kidney-derived macrophages infected with the intracellular pathogen, *Edwardsiella ictaluri,* and demonstrated that mAb CC41-reactive PBLs proliferated in this environment. As part of this project, a CC41 binding site was mapped to the D2-D3 interdomain hinge region of inhibitory LITR32.15 1.1a (Blackmon et al., 2020). Combined, these catfish studies demonstrated that IpLITRs are involved in cell-mediated immunity.

In this present study, we extend the studies by the Stafford laboratory and examine IpLITR-regulated phagocytosis in catfish cells. We take advantage of two anti-IpLITR mAbs, CC41 and 125.2, and demonstrate the effects of crosslinking subsets of inhibitory and activating LITRs using mAb-conjugated fluorescent microbeads in catfish T cell and macrophage cell lines.

2. Materials and methods

2.1. Experimental animals and leukocyte isolation

Outbred channel catfish were obtained from the Warmwater Aquaculture Research Unit in Stoneville, MS (USDA-Agriculture Research Service) and were individually housed as described in van Ginkel et al. (1992). All fish were maintained and handled according to institutional and national guidelines using protocols, #1128 and #1218, approved by the University of Mississippi Medical Center (UMMC) Institutional Animal Care and Use Committee (IACUC). Catfish were anesthetized with tricaine methanesulfonate (MS-222; Syndel), and blood was collected from the caudal vein using heparinized vacutainer tubes. Catfish peripheral blood leukocytes (PBLs) were isolated using Ficcoll-Hypaque (Accurate Chemical) density gradient centrifugation as described by Miller et al. (1994a).

2.2. Cell lines and cell culture

Catfish clonal cell lines and PBLs were cultured in AL-5 media or conditioned media at 27 °C with 5 % CO_2. AL-5 media consists of equal parts AIM V medium and L-15 medium (Invitrogen) adjusted to catfish tonicity and supplemented with 1 µg/mL $NaHCO_3$, 50 U/mL penicillin, 50 µg/mL streptomycin, 50 µM βME and supplemented with 5 % heat-inactivated pooled catfish serum (Miller, 1994a; Miller, 1994b). The conditioned media consists of AL-5 supplemented with 5 % filtered culture supernatant from catfish 28S.3 T cells and 5 % filtered culture supernatant from catfish 42TA macrophages. TS32.15 is a CTL clonal cell line, which requires weekly stimulation with irradiated allogenic 3B11 B cells (Stuge et al., 2000). Catfish clonal T cell lines, G14D and 28S.3 (Hogan et al., 1999; Wilson et al., 1998), and clonal B cell lines, 1G8 and 3B11 (Miller et al., 1994b; Wilson et al., 1997), are autonomous cell lines and do not require re-stimulation with allogeneic targets. The G14D γδ T cell line was established from PBLs isolated from a second-generation gynogenetic catfish (Hogan et al., 1999). The 42TA macrophage cell line is a non-clonal autonomous cell line that also contains some T cells that are required for the continuous growth of the culture (Vallejo et al., 1991). Mixed leukocyte cell cultures (MLCs) were established by culturing catfish PBLs in AL-5 media in the presence of irradiated allogenic 3B11 targets as described by Stuge et al. (1997). The MLCs were maintained by weekly restimulations with irradiated 3B11 B cells.

2.3. Monoclonal Abs

The mouse mAbs used in this study were anti-LITR, CC41 (IgG1κ), anti-LITR, 125.2 (IgG1κ), and anti-rainbow trout IgM, 1.14 (IgG1κ), which was used as an isotype control (Taylor et al., 2016; DeLuca et al., 1983). The monoclonal Ab 125.2 was obtained from BALB/c mice immunized with catfish TS32.15 CTLs using established protocols (Moretta et al., 1985; Campbell, 1991). Hybridomas were grown in media consisting of advanced Dulbecco's Modified Eagle Medium (DMEM, Gibco) with L-glutamine, 50 U/mL penicillin, 50 mg/mL streptomycin, and 15 % fetal bovine serum (FBS). Monoclonal antibody-containing culture supernatants were filtered (0.22 µm), aliquoted, and stored at − 20°C. Each mAb was affinity-purified using a Protein A-Sepharose 4B Conjugate column (Thermo Scientific), concentrated, and dialyzed into PBS. Monoclonal antibodies were stored at 4 °C until used.

2.4. Co-immunoprecipitations and western blotting

Anti-catfish LITR mAbs CC41 and 125.2 were used in co-immunoprecipitations to capture LITR target proteins. Briefly, 2×10^7 G14D γδ T cells and 2.5×10^7 cells from an MLC were surface biotinylated, lysed and immunoprecipitated using 125.2 and CC41, respectively. Both sets of cells were surface-biotinylated using the EZ-Link™ Sulfo-NHS-Biotinylation Kit (Thermo Scientific) according to the manufacturer's protocol with the exception that the buffers were adjusted to catfish tonicity (92 %). After harvesting, the cells were pelleted by centrifugation at 500 x g and resuspended in lysis buffer (10 mM Tris, 150 mM NaCl, 1 % NP-40, 1 Protease Inhibitor (Pierce) tablet, pH 7.4). The cells were lysed on ice for 15 min and precleared by centrifugation at 12,000 x g for 10 min. Prior to immunoprecipitation, 5 mg of Dynabeads M-270 (Invitrogen) were covalently coupled separately with 100 µg of affinity-purified mAb 125.2 or mAb CC41 according to the manufacturer's recommendations. The cleared lysates were then incubated with the coupled beads for one hour with end-over-end tilting at 4 °C. Proteins eluted from the beads were electrophoresed on reducing 10 % SDS-PAGE gels and transferred to PVDF membranes (EMD Millipore) for one hour at 100 V. To block non-specific binding, PVDF membranes were incubated in tris-buffered saline with 0.1 % Tween-20 (TBST) and 5 % BSA overnight at 4 °C. The membranes were washed three times in TBST and incubated with streptavidin-HRP (1:5000 TBST, 5 % BSA) for one hour at room temperature with gentle rocking. Afterwards, the membranes were again washed three times, and the biotinylated proteins were visualized using a SuperSignal West Pico Chemiluminescent Substrate kit (Thermo Scientific).

To determine if mAb 125.2 LITRs are tyrosine phosphorylated, G14D γδ T cells were treated with pervanadate. Briefly, 1.5×10^7 cells were surface biotinylated as above, suspended in pervanadate treatment solution (catfish tonicity phosphate buffered saline (cfPBS) adjusted with 0.1 mM Na_3VO_4 and 1.0 mM H_2O_2) and incubated for 30 min at 27 °C, 5 % CO_2. The G14D cells were then centrifuged, washed with cfPBS to remove the pervanadate, and then cell pellets were harvested for immunoprecipitation using the Capturem™ IP & Co-IP kit (Takara) and purified mAb 125.2. The G14D protein samples were separated using reducing 10 % SDS-PAGE, transferred to PVDF membranes, and visualized by western blot. Streptavidin-HRP was used to detect surface biotinylated proteins, and mouse anti-phosphotyrosine antibody (clone 4G10®, MilliporeSigma) followed by GAM IgG2b-HRP was used to detect phosphorylated tyrosines in pervanadate-treated samples.

To identify mAb 125.2 ligands, 1×10^9 G14D cells were immunoprecipitated using 125.2-coupled Dynabeads M-270 and the resulting proteins eluted from the Dynabeads were separated using reducing 10 % SDS-PAGE and visualized by Coomassie blue staining. Two protein bands of 120 kDa and 140 kDa were excised from the gel and submitted to Bioproximity Inc. for in gel-digestion and analysis by nanoLC-MS/MS as described in Taylor et al. (2016).

2.5. Bead conjugation

Fluorescent yellow-green, Fluoresbrite® YG Carboxylate beads (1.0 µm; Polysciences, Inc.) were conjugated to mAbs according to the manufacturer's "Carbodiimide" method protocol. For each antibody bead set, 50 mg of beads were washed and resuspended in 0.1 M 2-Morpholinoethanesulfonic acid sodium salt (MES) buffer. An equal volume of 2 % Carbodiimide was then added, and the bead suspension was mixed for 20 min at room temperature. The beads were then washed three times in 0.1 M MES buffer. After washing, the beads were resuspended in 1.2 mL of 0.2 M Borate buffer, and 200 µg of either affinity-purified mAb CC41, 125.2, or 1.14 were added to separate bead preparations. The bead preparations were incubated overnight at room temperature using an end-to-end mixer. Afterward, beads were collected by centrifugation and resuspended in 0.2 M Borate buffer; the unreacted sites on the beads were blocked by adding 50 µL of 0.25 M ethanolamine. The beads were then gently mixed for 30 min at room temperature, centrifuged, resuspended in 1 mL of 10 mg/mL BSA solution in 0.2 M Borate buffer, and incubated for 30 min at room temperature. The bead suspensions were then washed again with BSA solution. The antibody-conjugated beads were stored at 4 °C in 0.01 M phosphate buffer (pH 7.4), containing 1 % BSA, 0.1 % sodium azide, and 5 % glycerol.

The conjugation efficiency was evaluated spectrophotometrically (280 nm; $\varepsilon = 1.37$) by measuring the antibody left in the reaction supernatant after the beads were removed by centrifugation. In general, the conjugation efficiency was approximately 50 %, i.e., 100 µg of antibody was conjugated to the beads. The amount of antibody conjugated to the bead surface was also examined by flow cytometry using goat anti-mouse IgG1-APC (Southern Biotech) secondary antibody to ensure equivalent staining between different sets of mAb-conjugated beads.

2.6. Flow cytometry and phagocytosis assays

To establish staining profiles with mAbs CC41 and 125.2, 1×10^6 catfish leukocytes were incubated with 0.25 µg of mAb CC41, 125.2, or mAb1.14 (isotype control) in a volume of 100 µL for 15 min on ice. The cells were then washed in RPMI 1640 adjusted to catfish tonicity with 10 % deionized water (cfRPMI) and centrifuged at 500 x g for 5 min. After washing, the cells were resuspended in 100 µL of goat anti-mouse IgG1-PE (1:80 v/v in cfRPMI 1 % BSA; Southern Biotech) or goat anti-mouse IgG1-APC (1:100 v/v in cfRPMI 1 % BSA; Southern Biotech), incubated on ice for 15 min and washed again. The cells were resuspended in 500 µL of cfRPMI before flow cytometric analysis.

The phagocytosis assays in this study were performed using three channel catfish cell lines, G14D γδT cells, 28S.3 αβ T cells, 42TA macrophages, and catfish MLCs. Aliquots of each cell line or MLC were counted using a hemocytometer and stained with mAb 125.2 or CC41 to verify LITRs expression before each experiment. Briefly, a NovoCyte 3000 flow cytometer was used to determine the number of mAb-conjugated fluorescent beads per microliter. Aliquots of 1×10^6 cells were placed into flow cytometry tubes, washed, and incubated in a total volume of 1 mL cfRPMI 1 % BSA, with either CC41-, 125.2-, or 1.14-conjugated beads at bead-to-cell ratios of 2:1, 1:2, 1:4, 1:8. The bead and cell suspensions were incubated at 27 ^{o}C or on ice for 30 min, one hour, or two hours. After incubation and washing, the cells were counterstained with a goat anti-mouse IgG1-APC secondary antibody on ice for 30 min. The bead and cell suspensions were then washed, resuspended in 500 μL cfRPMI, and analyzed by flow cytometry. In the experiments that examined the effect of mAb CC41 on phagocytosis, 1×10^6 42TA macrophages were incubated with either 0.25 μg of mAb CC41 or 0.25 μg isotype control mAb 1.14 for one hour at room temperature. The 42TA macrophages were then washed four times in cfRPMI and uptake of 125.2- or CC41-conjugated fluorescent beads was examined after one hour at 27 ^{o}C by flow cytometry.

In these assays, total cell populations were gated, and cells associated with fluorescent YG beads were recorded in the FITC channel. The APC-conjugated secondary antibody made it possible to discriminate between cells with beads bound to their cell surface and cells that had phagocytosed their beads. Antibody-conjugated beads that were internalized were inaccessible to staining with the secondary antibody. The double negative gate was set based on the cell population that was not associated with beads and did not stain with the secondary antibody. The FITC positive, APC negative (FITC$^+$/APC$^-$) gate contained cells that had internalized beads but did not have surface-bound beads (Supplemental Fig. 1). Importantly, in this flow cytometry assay, cells with antibody-conjugated beads bound to their cell surface were counted in the double-positive quadrant even if they had phagocytosed several beads. Therefore, to minimize skewing of the results, the gates were set on cells associated with a single bead and used to calculate the percentage of cells that had internalized a bead.

2.7. *Confocal microscopy*

The catfish T cell lines, G14D or 28S.3, were incubated with mAb 125.2- or mAb CC41-conjugated beads at a cell-to-bead ratio of 1:5 for one hour at 27 ^{o}C, 5 % CO_2. Following bead uptake, the cells were stained for 20 min at room temperature with wheat germ agglutinin-Texas Red (WGA; 5 μg/mL; 561 nm; Invitrogen) which binds to cell surface glycoproteins. The cells were then washed in cfPBS, fixed with 2 % paraformaldehyde in cfPBS for 15 min at room temperature, and nuclei were stained with DAPI (405 nm; Thermo Scientific) at a concentration of 1 μg/mL for 5 min. The cells were then washed with cfPBS and mounted to slides with ProLong™ Diamond Antifade mountant (Invitrogen) for viewing on a Nikon C2+ confocal microscope. Beads were visualized using the FITC channel (488 nm), and images were captured at a resolution of 1024 × 1024 pixels (G14D) or 512 × 512 pixels (28S.3), with a Z-step of 0.5 μm and a total of 16 images per Z-stack.

2.8. *Statistical analysis*

Graphing and data analyses were performed using GraphPad Prism Software version 9.0.2 (Dotmatics). For graphs, error bars represent the mean with ± SD. To determine significance, data were analyzed using one-way ANOVA with multiple comparisons and Tukey's post-hoc test.

3. Results

3.1. *mAb 125.2 recognizes a subset of LITRs distinct from mAb CC41-reactive LITRs*

To determine if anti-LITR mAbs 125.2 and CC41 overlap in their staining profiles, catfish clonal and primary cell cultures were examined using flow cytometry. As shown in Fig. 1, catfish clonal T and B cell lines differ in their mAb 125.2 and mAb CC41 staining patterns. The catfish αβ T cell lines TS32.15 and 28S.3, each contain a small population of mAb 125.2-positive cells and stain brightly with mAb CC41 (Fig. 1A). In contrast, catfish clonal γδ G14D T cells stain brightly with mAb 125.2 and do not stain with mAb CC41. Both catfish clonal B cell lines, 1G8 and 3B11, are mAb 125.2-negative, while 3B11 stains brightly with mAb CC41 (Fig. 1B). The 42TA macrophage cell line, which contains a small population of T cells (2–10 %), and the MLC stain brightly with both mAb 125.2 and mAb CC41 (Fig. 1C). These findings suggest that mAb 125.2 recognizes ligands distinct from the LITR isoforms bound by mAb CC41. Therefore, to identify ligands recognized by mAb 125.2, immunoprecipitations were performed using G14D γδ T cells since these cells did not stain with mAb CC41 and stained more intensely with mAb 125.2 compared to our other catfish clonal cell lines. Immunoprecipitations of surface biotinylated G14D γδ T cells yielded several protein bands ranging in size from 26 to 150 kDa (Fig. 2A). This was expected since G14D expresses LITR transcripts that vary in length from 730 to 3000 bp (data not shown). The two protein bands of 120 kDa and 140 kDa were excised, subjected to nanoLC-MS/MS, and verified to contain LITR peptides. The 120 kDa protein yielded 30 unique LITR peptides, and 16 of these matched sequences within the extracellular Ig domains of LITR 2.2.5 (Fig. 2B, Supplementary Table 1). This activating LITR is expressed in PBL from a gynogenetic fish of the same lineage as the G14D γδ T cell line. The fainter 140 kDa band did not yield any peptides in addition to those obtained from the 120 kDa band. In comparison, mAb CC41 immunoprecipitations from MLCs predominantly selected proteins in the 115–150 kDa range (Fig. 2C). Since we had previously demonstrated that CC41-reactive LITRs were tyrosine phosphorylated following pervanadate treatment (Taylor et al., 2016), the signaling potential of 125.2-reactive LITRs in G14D γδ T cells was examined. G14D γδT cells were treated with pervanadate, lysed, and immunoprecipitated with mAb 125.2. Unlike CC41-reactive LITRs, 125.2-reactive LITRs were not phosphorylated (Fig. 2D). This data suggests that mAb 125.2 reacts with a subset of LITRs that have short cytoplasmic tails and signal through their associated adaptor proteins. The availability of two LITR-specific mAbs with different signaling capabilities provides the opportunity to explore LITR-mediated phagocytosis in catfish leukocytes.

3.2. *mAb 125.2-reactive LITRs mediate phagocytosis in catfish γδ T cells, while crosslinking CC41-reactive LITRs results in stalled phagocytosis*

Since mAbs 125.2 and CC41 differentially stain catfish G14D and 28S.3 T cells, it was possible to examine the independent effects of 125.2- and CC41-LITR crosslinking using flow cytometry. To establish LITR expression before each experiment, catfish G14D T cells were stained with mAb 125.2, and 28S.3 T cells were stained with mAb CC41. As shown in the histograms in Fig. 3A, 99.9 % of the G14D γδ T cells were mAb 125.2-positive, and 97.5 % of the 28S.3 T cells were CC41-positive. To examine LITR-mediated phagocytosis in these two autonomous T cell lines, G14D γδ T cells were incubated with mAb 125.2-conjugated 1.0 μm fluorescent beads, and 28 S.3 αβ T cells were incubated with mAb CC41-conjugated 1.0 μm fluorescent beads at a bead to cell ratio of 2:1. After one hour, the clonal γδ T cells and αβ T cells were stained using an APC-conjugated goat anti-mouse IgG1 secondary antibody to discriminate between cells associated with surface-bound fluorescent beads and cells that had internalized the beads. Approximately 6.6 % of all G14D γδ T cells and 14.3 % of 28S.3 αβ T cells had either

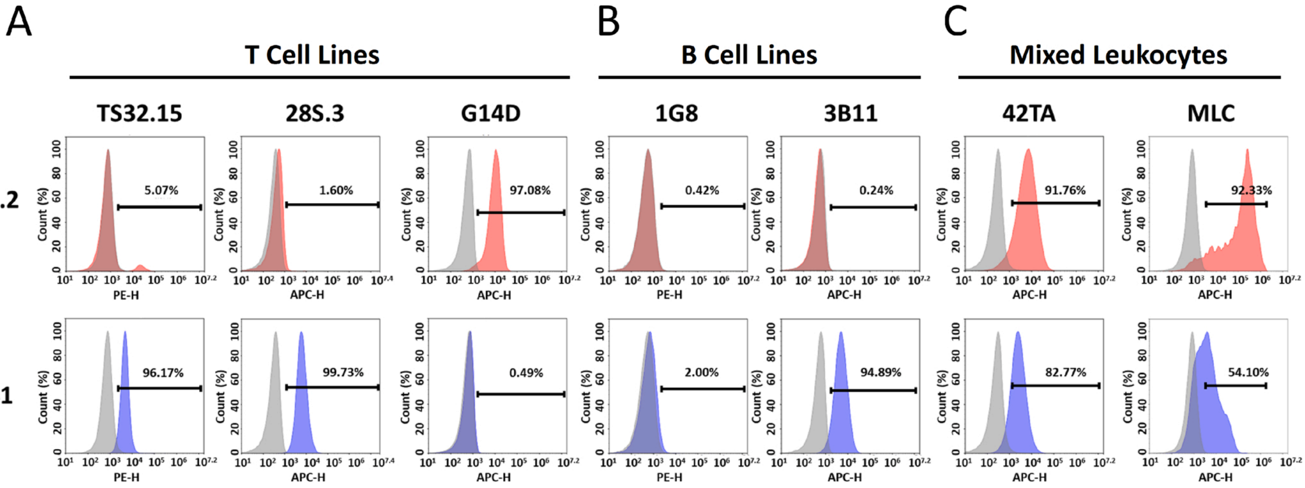

Fig. 1. Anti-LITR mAbs 125.2 and CC41 differentially stain catfish clonal αβ and γδ T cells, clonal 3B11 and 1G8 B cells, 42TA macrophages and catfish mixed leukocyte cultures (MLCs). Flow cytometry profiles of catfish clonal (A) TS32.15 αβ T cells, 28S.3 αβ T cells, and G14D γδ T cells, (B) 1G8 and 3B11 B cells, and (C) 42TA macrophages are compared with profiles from a mixed leukocyte culture (MLC) obtained from catfish PBLs co-cultured with irradiated 3B11 B cells for 6 days. The normalized histograms show the clonal cell lines and an MLC staining with mAbs 125.2 (in red) and CC41 (in blue) followed by either PE- or APC-conjugated goat anti-mouse IgG. The percentages of positive cells relative to staining with the anti-rainbow trout IgM 1.14 isotype control (in grey) are indicated.

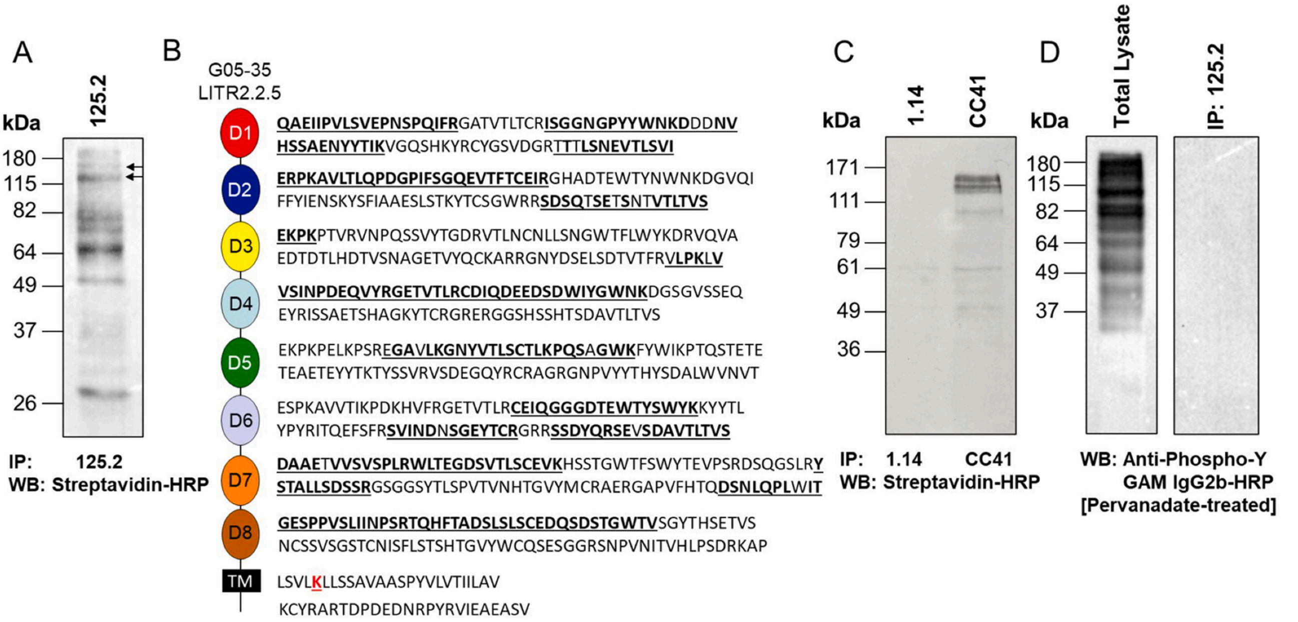

Fig. 2. mAb 125.2 binds activating LITRs. (A) 5 × 10^7 surface-biotinylated G14D T cells, were lysed, and immunoprecipitated using mAb 125.2-conjugated M-270 Dynabeads. The immunoselected proteins were then electrophoresed by reducing SDS-PAGE, transferred to PVDF membranes, and visualized by western blot using Streptavidin-HRP. In parallel, an immunoprecipitation was performed using 1 × 10^9 G14D T cells and mAb 125.2-conjugated M-270 Dynabeads. Immunoselected proteins were separated by reducing SDS-PAGE and visualized by Coomassie blue staining (data not shown). The corresponding protein bands indicated by the arrows were subjected to nanoLC-MS/MS. (B) A schematic of LITR 2.2.5 is presented on the right, and the positively charged lysine residue in the TM sequence is indicated in red. The identified LITR peptides that match the LITR2.2.5 sequence are in bold and underlined. (C) 2.5 × 10^7 cells from a mixed leukocyte culture were treated as in (A) and immunoprecipitated with mAb CC41. (D) 1.5 × 10^7 G14D T cells were treated with pervanadate, lysed, and either electrophoresed directly as in (A) or immunoprecipitated with 125.2 and separated by SDS-PAGE. The proteins were then transferred to PVDF membranes, and phosphorylated proteins were visualized by western blot. The total cell lysates include tyrosine phosphorylated proteins (left) and the 125.2 immunoselected proteins which were not phosphorylated (right).

bound or fully internalized one to four beads (Fig. 3B). This suggests that the slightly weaker staining observed with mAb CC41 on 28S.3 T cells did not negatively impact their ability to bind beads. In the flow cytometric analysis, cells in the double-negative lower left quadrant are not phagocytic, while cells in the single positive ($FITC^+/APC^-$) lower right quadrant have internalized all the associated beads (Fig. 3C). Also, it should be noted that the double positive ($FITC^+/APC^+$) upper right quadrant contains a mixed population of cells with surface-bound fluorescent beads, some of which are non-phagocytic and others that have internalized beads. Therefore, in our analyses, we used a high cell-to-bead ratio of 2:1 and gated on cells associated with only one fluorescent bead to clearly discriminate between surface-bound and fully internalized beads. Still, it is likely that we are underestimating the phagocytic activities due to this conservative gating strategy. When G14D γδ T cells were incubated at 27 °C, 40.96 % of the cells associated with one 125.2-conjugated bead had internalized the bead (Fig. 3D). In

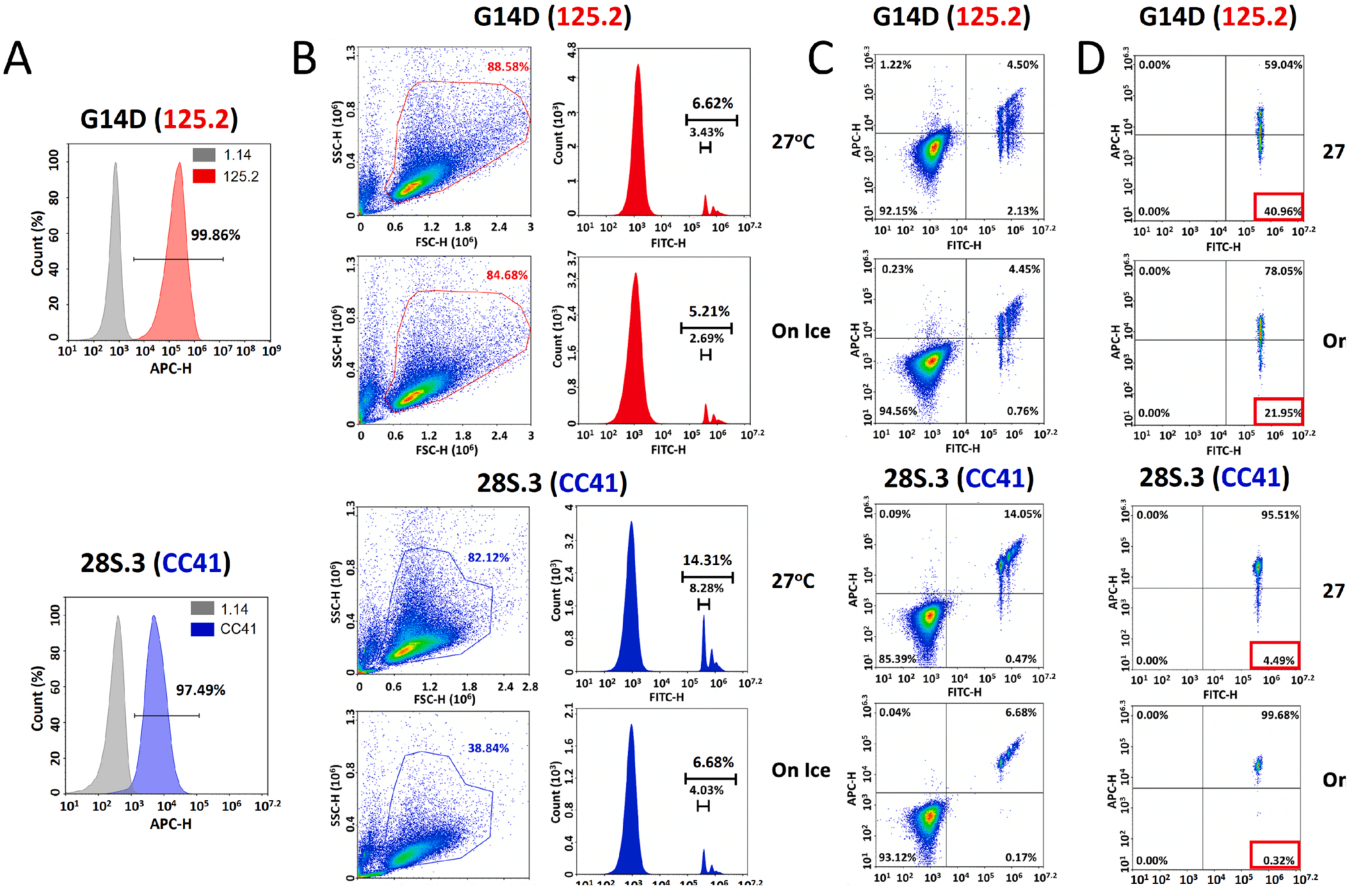

Fig. 3. LITR-crosslinking on G14D with mAbs 125.2 and CC41 result in different phagocytic phenotypes. (A) Catfish clonal G14D γδ T cells and 28S.3 αβ T cells were stained with anti-LITR mAbs 125.2 (red) and CC41 (blue), respectively, to confirm LITR expression. The isotype control mAb 1.14 is in gray. (B) In parallel, G14D and 28S.3 T cells were separately incubated with mAb 125.2-conjugated (red) or CC41-conjugated (blue) 1.0 μm fluorescent beads at a cell-to-bead ratio of 2:1 for 1 h at 27 °C (top panels) or on ice (bottom panels). The cells were then counter-stained with goat anti-mouse IgG1-APC secondary antibody to discriminate between cells with surface-bound fluorescent beads and cells that had internalized the beads. Scatter profiles show the gated cell populations, and histograms indicate the percentages of cells associated with a single bead. (C) Double-staining discriminates between cells that are not associated with any beads in the double-negative APC$^-$/FITC$^-$ lower left quadrant and cells associated with YG fluorescent beads in the upper right and lower right quadrants. Cells in the lower right quadrant have internalized all the associated beads and are APC$^-$, while cells in the double-positive upper right quadrant contain a mixed population of cells with beads bound to their surface, even if several beads are internalized. (D) To minimize skewing of the results, percentages of cells that had internalized beads were analyzed based on cells associated with a single bead.

contrast, only 4.49 % of the 28S.3 T cells associated with one CC41-conjugated bead internalized the bead. In comparison, when catfish T cells were incubated on ice, the internalization of 125.2-conjugated beads by G14D was reduced to 21.95 %, and the uptake of CC41-conjugated beads by 28S.3 T cells was reduced to 0.32 %. Combined, these results suggest that crosslinking with mAb 125.2 mediates

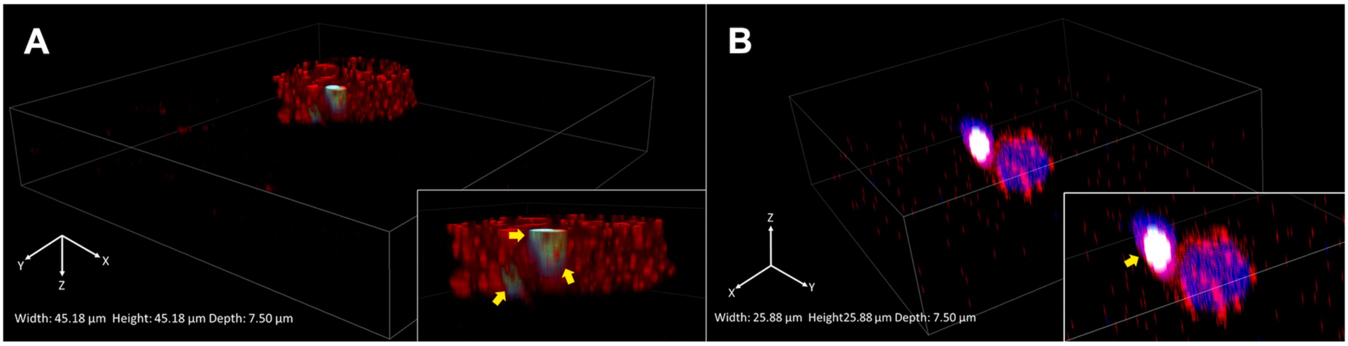

Fig. 4. G14D γδ T cells phagocytose mAb 125.2-conjugated beads, while CC41-beads remain at the surface of 28S.3 T cells. (A) G14D T cells were incubated with mAb 125.2-conjugated 1.0 μm beads for 1 h at 27 °C, 5 % CO_2 at a cell-to-bead ratio of 1:5. The cells were stained with wheat germ agglutinin-Texas Red (WGA) at a concentration of 5 μg/mL for 20 min at room temperature. The G14D cells were then washed and fixed with 2 % paraformaldehyde in catfish tonicity PBS for 15 min at room temperature and stained with DAPI at a concentration of 1 μg/mL for 5 min (data not shown). Cells were mounted to slides using Prolong Diamond Antifade mountant and viewed by confocal microscopy. Yellow arrows indicate the three beads that were taken up by a single G14D cell. (B) 28S.3 T cells were incubated with mAb CC41-conjugated beads for 1 h as in (A), and the yellow arrow indicates a single captured bead displayed on the surface of a 28S.3 T cell.

phagocytosis more efficiently than mAb CC41-crosslinking.

To visualize the phenotypic differences in mAb 125.2- and mAb CC41-mediated bead interactions, confocal microscopy was performed with G14D and 28S.3 T cells. In agreement with the flow cytometry-based phagocytosis assays above, confocal images of G14D cells showed that these γδ T cells are able to bind and phagocytose mAb 125.2-conjugated fluorescent 1 μm beads (Fig. 4). However, when 28S.3 αβ T cells were examined after one hour, mAb CC41-conjugated beads appeared to be stalled at the plasma membrane. Overall, cross-linking mAb 125.2-reactive LITRs mediated phagocytosis, while cross-linking LITRs with mAb CC41 resulted only in a capturing phenotype.

3.3. Phagocytosis mediated by 125.2-reactive LITRs in 42TA macrophages is inhibited by CC41-reactive LITRs

We next examined IpLITR-mediated phagocytosis by 42TA macrophages. This catfish cell line consistently stains with both mAb 125.2 and mAb CC41. When 42TA macrophages were stained separately with mAb 125.2 or mAb CC41, the percent of positive cells in different cultures ranged from 77 % to 95 % and from 78 % to 99 %, respectively. In two-color flow cytometry, using Zenon-FITC labeled mAb 125.2 and APC-conjugated mAb CC41, 94.7 % of 42TA cells were positive for both mAbs (Fig. 5A). Notably, the ability of 42TA macrophages to associate with either 125.2- or CC41-conjugated 1.0 μm fluorescent beads is approximately the same (18.53 % vs. 16.03 %) as shown in the histograms presented in Fig. 5B (left panels). However, there is a clear difference in the uptake of the 125.2- and CC41-conjugated beads. After one hour at 27 °C, 21.76 % of the 42TA cells that had bound a single 125.2-conjugated bead had completely internalized that bead and were negative for goat anti-mouse IgG-APC (Fig. 5B, right panel). In contrast, only 3.75 % of the 42TA cells associated with a single CC41-conjugated bead had engulfed their target. These results were reproducible and significant (Fig. 6A). Beads conjugated with the isotype control were not phagocytosed (Supplemental Fig. 2). Combined, the flow cytometry studies of IpLITR-mediated phagocytosis in G14D γδ T cells, 28S.3 αβ T cells, and 42TA macrophages provide evidence that mAb 125.2 recognizes activating IpLITRs, while mAb CC41 preferentially binds to inhibitory LITRs.

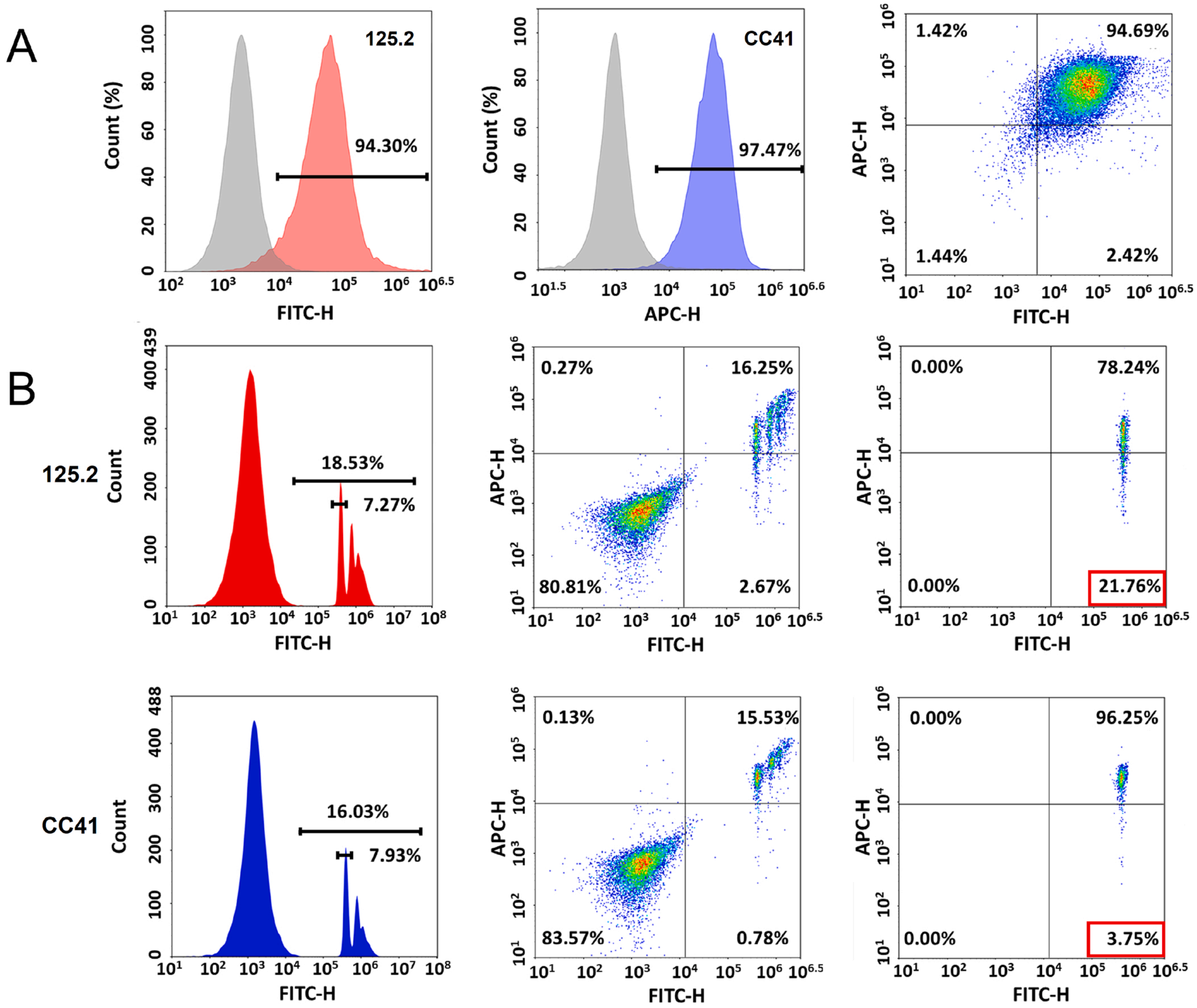

Fig. 5. LITR-reactive mAbs 125.2 and CC41 stain 42TA macrophages, only mAb 125.2-mediates efficient phagocytosis. 42TA is a monocyte/macrophage cell line that contains a few T cells. (A) Individual staining and double staining of 42TA with mAb 125.2 and CC41. (B) 42TA cells were incubated with CC41- or 125.2-conjugated beads at a cell-to-bead ratio of 1:5 for 1 h at 27 °C. Afterward, 42TA cells were stained with goat anti-mouse IgG1-APC for 15 min on ice, washed, and analyzed by flow cytometry. N = 5, $p < 0.001$.

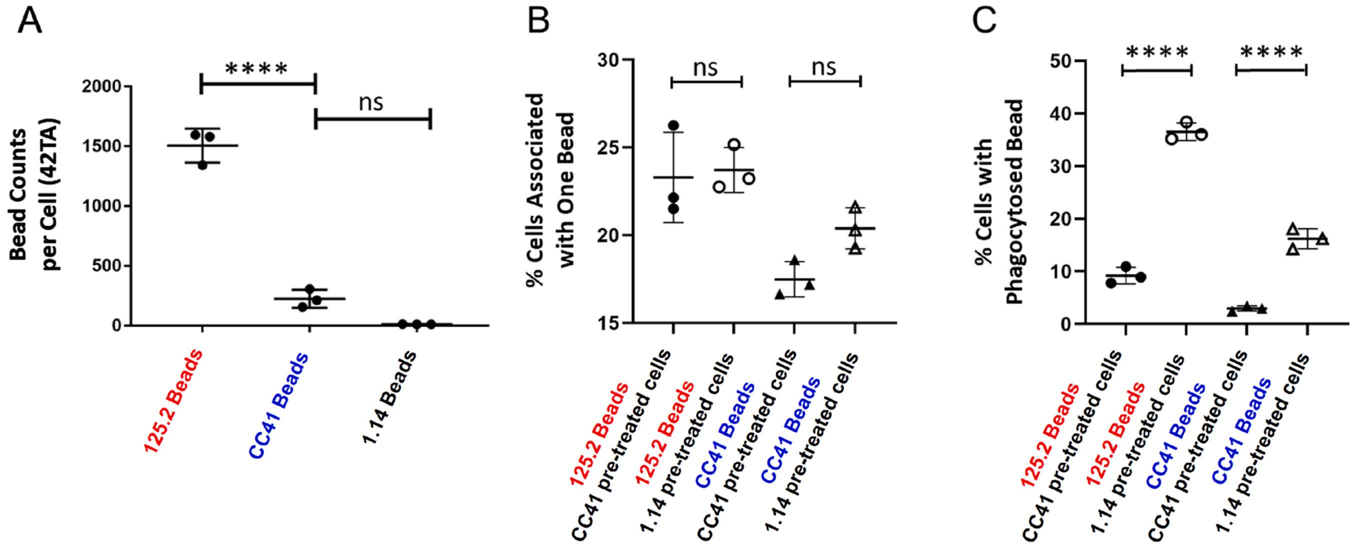

Fig. 6. Pre-treatment of 42TA macrophages with mAb CC41 inhibits mAb 125.2-mediated phagocytosis. (A) 42TA macrophages were incubated with either mAb 125.2-, CC41-, or 1.14-conjugated beads for 1 h at 27 °C 5 % CO_2 at a cell-to-bead ratio of 1:5. Bead uptake was examined by flow cytometry. Only cells that had phagocytosed a single bead were counted ($N = 3$). Prior to statistical analysis, the data were normalized to 100,000 events to correct for variance in live cell counts between the samples. The uptake of 125.2-conjugated beads was significantly higher ($p < 0.0001$) compared to the uptake of CC41-conjugated beads. The difference in uptake between the isotype control 1.14-conjugated beads and CC41-conjugated beads was not significant. (B, C) 42TA macrophages were pretreated with either 0.25 μg isotype control mAb 1.14 (open symbols ○, △) or 0.25 μg of mAb CC41 (solid symbols •, ▲) for 1 h at room temperature. The cells were then washed four times to remove antibodies, and uptake of 125.2- or CC41-conjugated fluorescent beads was examined after 1 h at 27 °C. (B) Pretreatment with mAb CC41 did not significantly affect the ability of 42TA macrophages to associate with 125.2-conjugated beads. (C) Pretreatment with mAb CC41 significantly ($p < 0.0001$) reduced the bead uptake compared to pre-treatment with the mAb 1.14 isotype control.

To better understand this interplay between inhibitory and activating LITRs in the context of phagocytosis, we next examined the consequences of cross-linking with mAb CC41 as a pretreatment before adding 125.2-conjugated or CC41-conjugated fluorescent beads. Previously we had demonstrated that crosslinking CC41-reactive LITRs on cytotoxic cells reduced the killing of antigen-specific target cells (Taylor et al., 2016). Therefore, it was predicted that mAb CC41 cross-linking of inhibitory IpLITRs would reduce 125.2-mediated bead uptake. Briefly, 42TA macrophages were incubated for one hour at room temperature with either 0.25 μg of mAb CC41 or 0.25 μg of the isotype control mAb 1.14. The macrophages were then washed and assayed for the ability to engulf 125.2- or CC41-conjugated fluorescent beads (Fig. 6B). Importantly, pretreatment with mAb CC41 did not significantly affect the ability of 42TA macrophages to bind 125.2-conjugated beads, however it did impact the binding of CC41-conjugated beads. Notably, uptake of 125.2-conjugated beads by mAb CC41-treated 42TA macrophages was significantly reduced ($p < 0.0001$) as compared to uptake by 42TA macrophages pre-treated with the isotype control, mAb 1.14 (Fig. 6C). This finding suggests that an inhibitory signal generated by mAb CC41 was able to override the activating LITR signal mediated by mAb 125.2.

In summary, we have identified an anti-LITR mAb 125.2 that binds to activating LITRs and used this antibody to demonstrate IpLITR-mediated phagocytosis in catfish γδ T cells and macrophages. Moreover, cross-linking mAb CC41-reactive LITRs resulted in low-level uptake and inhibition of mAb 125.2-mediated phagocytosis. These findings are consistent with mAb CC41 binding to inhibitory LITRs. This is the first time LITR-mediated phagocytosis has been demonstrated in the catfish model.

4. Discussion

In this study, we took advantage of two of our anti-LITR mAbs and examined the effects of crosslinking their respective ligands on catfish leukocytes. Overall, the three key findings from this work demonstrate that 1) IpLITR-specific mAb 125.2 recognizes a distinct subset of activating LITR isoforms that lack phosphotyrosines in their CYTs and is expressed on G14D γδ T cells; 2) mAb 125.2-reactive LITRs mediate phagocytosis in catfish γδ T cells and macrophages, and 3) mAb CC41-reactive LITRs inhibit phagocytosis mediated by 125.2-reactive LITRs. Together, these results represent the first direct demonstration of LITR-mediated phagocytosis in catfish leukocytes and validate the findings of LITR-mediated regulation obtained in mammalian cell lines (Cortes et al., 2014; Lillico et al., 2015., 2018; Fei et al., 2020). Even so, it is important to note that LITRs may regulate additional cellular responses that may share components of their signaling pathways. For example, LITR signaling may mediate secretion of inflammatory cytokines, initiate the respiratory burst, and trigger cellular degranulation. It is also likely that LITRs in different cell types mediate different functions.

Previously, we characterized two anti-LITR mAbs, CC34 and CC41, that recognize overlapping subsets of LITRs expressed on catfish leukocytes. Notably, mAb CC41-reactive LITRs were considered a marker for catfish cytotoxic cells based on the findings that 1) $CC41^+$ PBLs isolated from a CCV-immunized fish efficiently killed CCV-infected target cells, while CC41-negative PBLs did not kill the infected-targets, 2) 90 % of $CC41^+$ PBL isolated from a CCV-immunized fish expressed perforin in FlowRNA analysis, and 3) the $CC41^+$ cell population increased after immunization with CCV-infected syngeneic cells. Furthermore, pretreatment of MLC-derived effector cells with mAb CC41 reduced the cytotoxic activity by 40 % (Taylor et al., 2016). Together these findings suggested that CC41-reactive LITRs, like other paired receptors i.e., LILRs and KIRs, have a direct role in target cell recognition and regulation of cytotoxic activity. We later determined that both mAbs CC34 and CC41 recognize epitopes within the D2-D3 interdomain hinge region of IpLITR32.15 1.1a (Blackmon et al., 2020). This LITR consists of seven extracellular Ig domains, a TM, and a 125 amino acid long CYT with six tyrosine residues. The three membrane-proximal tyrosines are not a part of any classical regulatory motif, while the three membrane-distal tyrosines each form a part of an ITIM (VxYxxI) or an ITSM-like motif (TxYxxL).

In this study, we identified a third LITR-specific mAb, 125.2, which immunoselects a range of proteins from 26 to 150 kDa expressed on catfish clonal G14D γδ T cells (Fig. 2A). Moreover, mAb 125.2 was specific for activating LITRs since these 125.2 reactive LITR proteins were not tyrosine phosphorylated after pervanadate treatment. Two of the immunoprecipitated protein bands, 120 kDa and 140 kDa, were verified by nanoLC-MS/MS to contain LITR peptides. Specifically, the 120 kDa protein yielded overlapping peptides that matched sequences from the eight extracellular Ig domains of LITR 2.2.5 (Fig. 2B). This activating LITR was expressed in PBL from a gynogenetic fish of the same lineage as the G14D γδ T cell line. That only ten of the peptides derived from the 120 kDa protein band were identical to the peptides obtained from TS32.15 CTLs using CC41 also supports that mAb 125.2 reacts with a different LITR subset.

Since LITRs comprise such a large family of receptors with unknown ligands, most functional studies have focused on intracellular signaling events mediated by activating IpLITR2.6b and inhibitory IpLITR1.1b. The signaling potentials of these prototypic LITRs have been well characterized in mammalian fibroblasts and myeloid cells by using epitope-tagged proteins, co-immunoprecipitation, and microscopy (Montgomery et al., 2012; Cortes et al., 2014; Zwozdesky et al., 2017; Lillico et al., 2015, 2018). One of the most striking findings from these imaging studies was the IpLITR1.1b-mediated stalled phagocytic phenotype observed in the transfected rat basophils (RBL-2H3). Interestingly, the inhibitory IpLITR1.1b transfected basophils constitutively generated filopodia and sampled their environment without any stimulation. Moreover, live cell imaging revealed actin-rich membrane protrusions that captured the antibody-conjugated beads in phagocytic cup-like structures that stalled at the cell membrane (Lillico et al., 2018). In contrast, transfection with the activating IpLITR2.6b/IpFcRγ-L construct resulted in effective phagocytosis of antibody-conjugated beads, however filopodia bead captures were not observed. That the inhibitory receptor LITR1.1b regulated F-actin dynamics was unexpected and led the authors to the idea that the IpLITR1.1b CYT is constitutively phosphorylated and pre-associated with intracellular components of the cytoskeletal machinery (Lillico et al., 2018). Support for this idea came from the finding that adaptor protein, non-catalytic region of tyrosine kinase (Nck) constitutively co-localized with IpLITR1.1b within the filopodia of the transfected basophils (Lillico et al., 2020). Similarly, in our study, G14D γδ T cells readily phagocytosed their targets after activating LITRs were crosslinked with mAb 125.2-conjugated beads. In contrast, after crosslinking inhibitory LITRs, more than 95 % of the CC41-conjugated beads remained on the cell surface of 28S.3 αβ T cells (Fig. 3). This discrepancy in phagocytic phenotypes was also confirmed by confocal microscopy, where complete internalization of 125.2 beads and stalled phagocytosis of CC41-conjugated beads could clearly be distinguished (Fig. 4). This capturing of CC41-conjugated beads is reminiscent of the phagocytic cup-like structures observed by electron microscopy with LITR1.1b in RBL-2H3 basophils (Lillico et al., 2018). Since IpLITR32.15 1.1a, the target of mAb CC41, and IpLITR1.1b, the prototypic LITR used in RBL-2H3 cells, have very similar CYTs that only differ by three amino acids, these phenotypic similarities were expected.

Notably, the uniform co-expression of 125.2- and CC41-reactive LITRs in catfish 42TA macrophages allowed us to examine the inhibitory function of CC41-reactive LITRs in LITR-mediated phagocytosis. As shown in Fig. 5, anti-LITR mAbs 125.2 and CC41 mediate the same phagocytic phenotypes in 42TA as in the catfish T cell lines. As expected, mAb 125.2-conjugated beads were internalized, while CC41 promoted a capturing phenotype. However, when 42TA macrophages were pre-incubated with mAb CC41, phagocytosis of mAb125.2-conjugated beads was reduced by 75 % as compared to pretreatment with the control mAb 1.14 ($p < 0.0001$; see Fig. 6C). In 2020, Fei et al. examined the crosstalk of activating and inhibitory LITRs in phagocytosis inhibition by co-expressing epitope-tagged IpLITR2.6b/IpFcRγ-L and IpLITR1.1b in AD293 cells. By using a combination of site-directed mutagenesis and IpLITR crosslinking, it was demonstrated that sustained inhibition required the combined recruitment of the inhibitory kinase, Csk, and the phosphatase, SHP-2, to specific tyrosines within the IpLITR1.1b CYT. Based on their findings, the authors proposed that signaling through activating LITRs is required to initiate the subsequent inhibitory pathway, i.e., the inhibitory receptors must first be “activated” by Src family kinases to recruit inhibitory kinases and phosphatases (Csk and SHP-2; Fei et al., 2020). Here in this study, it is interesting that crosslinking inhibitory CC41-reactive LITRs as a pretreatment resulted in significant phagocytosis inhibition even though activating LITRs were not previously crosslinked. It may be that inhibitory LITRs like IpLITR32.151.1a and IpLITR1.1b are basally phosphorylated in catfish cells. Alternatively, mAb CC41 may bind to both activating and inhibitory LITRs, albeit with different affinities. If true, this would allow for the co-crosslinking of activating and inhibitory LITRs, which would facilitate crosstalk between these receptors. In the study by Taylor et al. (2016), pretreatment of MLC effector cells with mAb CC41 led to a 40 % reduction in the cytotoxic activity against virus-infected target cells. At the time, it was proposed that the inhibition could be due to mAb CC41 sterically hindering the interaction between the effector cells and the target cells; it was also considered that mAb CC41 might bind to inhibitory receptors and reduce target cell killing. However, at the time, these alternatives could not be discerned using cytotoxic assays. In the 42TA phagocytosis assay, we could determine that the binding of mAb 125.2-conjugated beads was unaffected by the mAb CC41 pretreatment and that inhibition likely was due to intracellular signaling events.

Although not the focus of this current study, we confirmed that catfish clonal G14D γδ T cells are phagocytic and that phagocytosis can involve IpLITRs. Interestingly, human peripheral blood γδ T cells are phagocytic and function as professional antigen-presenting cells (Brandes et al., 2005, 2009). For example, in one study, γδ T cells phagocytosed opsonized particulate antigens via the FcR, CD16, and processed and presented these antigens on MHC class II to naïve CD4 T cells (Wu et al., 2009). To our knowledge, phagocytosis by teleost γδ T cells has only been reported in zebrafish. These γδ T cells can phagocytose particulate and soluble antigens and present peptides to CD4 T cells. Moreover, the depletion of the γδ T cell population in zebrafish significantly reduced antigen-specific IgM and IgZ titers (Wan et al., 2017). Since catfish G14D γδ T cells and 28S.3 αβ T cells, in contrast to catfish clonal NK cells, uniformly express high levels of MHC class II (Moulana et al., 2008), it seems likely that activated catfish γδ T cells, in addition to γδ T cells, are also capable of phagocytosis. However, the low expression levels of mAb 125.2-reactive LITRs in our γδ T cell lines precluded examining LITR-mediated phagocytosis in these cells. Also, because none of our clonal B cell lines were reactive with mAb 125.2, which is specific for activating LITRs, LITR-mediated phagocytosis by B cells could not be examined. However, it is interesting that our two catfish B cell lines differentially stain with mAbs that recognize inhibitory LITRs, including LITR32.151.1a. The 3B11 B cells stain brightly with mAb CC41 and do not stain with mAb CC34, while 1G8 B cells only stain with mAb CC34 (data not shown). These findings raise the question of whether IpLITRs can regulate B cell receptor signaling. In humans, the inhibitory Fc_{γ}RIIb (CD32B) and FcRL3–5 are expressed in subpopulations of B cells, and these receptors are known to modulate B cell activation (Karnell et al., 2014; Tolnay, 2022). Like traditional FcRs, human FCRL3, FCRL4, and FCRL5 bind secretory-IgA, dimeric IgA, and IgG, respectively. It is proposed that these FCRLs distinguish the mucosal and systemic origin of immune complexes and help regulate memory B cell responses at mucosal sites (Tolnay, 2022). The syntenic and phylogenetic relationships of LITRs with FCRLs also suggest that they may have similar functions. Notably, IpLITR2.6b, IpLITR1.1b, and IpLITR32.151.1a do not bind to catfish IgM (data not shown); even so, we cannot rule out that other LITRs in this large receptor family may bind immunoglobulins. While our goal is to identify ligands for activating and inhibitory LITRs, determining the ligands for individual paired receptors in any species is challenging. Most mammalian paired receptors bind several host- and pathogen-derived molecules (Barclay and Hatherley, 2008; Burshtyn and Morcos, 2016; Barrow et al., 2019; Levi-Schaffer and Mandelboim, 2018). For example, LILRs interact with diverse types of ligands, including classical and nonclassical MHC molecules. In addition, LILRs are also known to bind intact pathogens, including *Staphylococcus aureus, Escherichia coli,* and *Helicobacter pylori* (Burshtyn and Morcos, 2016).

Overall, our studies have demonstrated that LITRs are involved in regulating phagocytosis, as well as cytotoxic responses in channel catfish. The availability of long-term catfish cell lines that express high levels of distinct LITR subsets made it possible to examine the independent effects of crosslinking CC41-reactive inhibitory LITRs and 125.2-reactive activating LITRs. As such, our current findings complement LITR signaling studies performed in mammalian cell lines and set the stage for exploring the consequences of LITR-mediated phagocytosis in catfish leukocytes. Building on this work, we believe it will be possible to examine the intracellular and biochemical consequences of receptor crosslinking in different types of leukocytes in catfish.

Funding

This work was supported by the U.S. Department of Agriculture, National Institute of Food and Agriculture Predoctoral Fellowship USDA-NIFA 2020-67034-31895 (J. C.), 2022-67011-36580 (K.L.F), and the National Science Foundation Grant IOS-1655419.

CRediT authorship contribution statement

Jonathan Crider: Investigation, Validation, Formal analysis, Writing – original draft, Visualization. **Melanie Wilson:** Conceptualization, Methodology, Funding acquisition, Supervision, Writing – review & editing. **Kristianna L. Felch:** Investigation. **Rebecca A. Dupre:** Investigation, Resources. **Sylvie M.A. Quiniou:** Methodology, Resources, Funding acquisition, Supervision. **Eva Bengtén:** Conceptualization, Methodology, Visualization, Funding acquisition, Supervision, Writing – review & editing.

Declarations of interests

None.

Data Availability

Data will be made available on request.

Acknowledgements

The authors would like to thank the Mississippi Center for Supercomputing Research (MCSR) for access to computational resources through their facility at the University of Mississippi, Oxford, MS, USA. The authors would also like to thank Dr. Jorge Vidal (University of Mississippi Medical Center) for his help with confocal imaging. Research reported in this publication was supported by the National Institute of General Medical Sciences of the National Institutes of Health under Award Number P20GM121334. The content is solely the responsibility of the authors and does not necessarily represent the official views of the National Institutes of Health.

Appendix A. Supporting information

Supplementary data associated with this article can be found in the online version at doi:10.1016/j.molimm.2022.12.009.

References

Akkaya, M., Barclay, A.N., 2013. How do pathogens drive the evolution of paired receptors? Eur. J. Immunol. 43 (2), 303–313. https://doi.org/10.1002/eji.201242896.

Barclay, A.N., Van den Berg, T.K., 2014. The interaction between signal regulatory protein alpha (SIRPα) and CD47: structure, function, and therapeutic target. Annu. Rev. Immunol. 32, 25–50. https://doi.org/10.1146/annurev-immunol-032713-120142.

Barclay, N.A., Hatherley, D., 2008. The counterbalance theory for evolution and function of paired receptors. Immunity 29 (5), 675–678. https://doi.org/10.1016/j.immuni.2008.10.004.

Barrow, A.D., Martin, C.J., Colonna, M., 2019. The natural cytotoxicity receptors in health and disease. Front. Immunol. 10, 909. https://doi.org/10.3389/fimmu.2019.00909.

Billadeau, D.D., Leibson, P.J., 2002. ITAMs versus ITIMs: striking a balance during cell regulation. J. Clin. Invest. 109, 161–168. https://doi.org/10.1172/JCI14843.

Blackmon, L.E., Quiniou, S.M.A., Wilson, M., Bengtén, E., 2020. Catfish lymphocytes expressing CC41-reactive leukocyte immune-type receptors (LITRs) proliferate in response to *Edwardsiella ictaluri* infection in vitro. Dev. Comp. Immunol. 106, 103610 https://doi.org/10.1016/j.dci.2020.103610.

Borrego, F., 2013. The CD300 molecules: an emerging family of regulators of the immune system. Blood 121 (11), 1951–1960. https://doi.org/10.1182/blood-2012-09-435057.

Boudinot, P., Zou, J., Ota, T., Buonocore, F., Scapigliati, G., Canapa, A., Cannon, J., Litman, G., Hansen, J.D., 2014. A tetrapod-like repertoire of innate immune receptors and effectors for coelacanths. J. Exp. Zool. B Mol. Dev. Evol. 322 (6), 415–437. https://doi.org/10.1002/jez.b.22559.

Brandes, M., Willimann, K., Moser, B., 2005. Professional antigen-presentation function by human gammadelta T cells. Science 309 (5732), 264–268. https://doi.org/10.1126/science.1110267.

Brandes, M., Willimann, K., Bioley, G., Levy, N., Eberl, M., Luo, M., Tampe, R., Levy, F., Romero, P., Moser, B., 2009. Cross-presenting human γδ T cells induce robust CD8$^+$ αβ T cell responses. Proc. Natl. Acad. Sci. USA 106, 2307–2312. https://doi.org/10.1073/pnas.0810059106.

Brandes, M., Willimann, K., Bioley, G., Lévy, N., Eberl, M., Luo, M., Tampé, R., Lévy, F., Romero, P., Moser, B., 2009. Cross-presenting human gammadelta T cells induce robust CD8+ alphabeta T cell responses. Proc. Natl. Acad. Sci. USA 106, 2302–2312. https://doi.org/10.1073/pnas.0810059106.

Burshtyn, D.N., Morcos, C., 2016. The expanding spectrum of ligands for leukocyte Ig-like receptors. J. Immunol. 196 (3), 947–955. https://doi.org/10.4049/jimmunol.1501937.

Campbell, A.M., 1991. Monoclonal antibody and immunosensor technology: the production and application of rodent and human monoclonal antibodies. In: Vliet, P. Cvd (Ed.), Laboratory Techniques in Biochemistry and Molecular Biology. Elsevier, New York, pp. 1–47.

Clem, L.W., Bly, J.E., Wilson, M., Chinchar, V.G., Stuge, T., Barker, K., Luft, C., Rycyzyn, M., Hogan, R.J., van Lopik, T., Miller, N.W., 1996. Fish immunology: the utility of immortalized lymphoid cells–a mini review. Vet. Immunol. Immunopathol. 54 (1–4), 137–144. https://doi.org/10.1016/s0165-2427(96)05682-6.

Cortes, H.D., Montgomery, B.C., Verheijen, K., Garcia-Garcia, E., Stafford, J.L., 2012. Examination of the stimulatory signaling potential of a channel catfish leukocyte immune-type receptor and associated adaptor. Dev. Comp. Immunol. 36, 62–73. https://doi.org/10.1016/j.dci.2011.06.004.

Cortes, H.D., Lillico, D.M.E., Zwozdesky, M.A., Pemberton, J.G., O'Brien, A., Montgomery, B.C., Wiersma, L., Chang, J.P., Stafford, J.L., 2014. Induction of phagocytosis and intracellular signaling by an inhibitory channel catfish leukocyte immune-type receptor: evidence for immunoregulatory receptor functional plasticity in teleosts. J. Innate Immun. 435–455. https://doi.org/10.1159/000356963.

Daëron, M., Jaeger, S., Du Pasquier, L., Vivier, E., 2008. Immunoreceptor tyrosine-based inhibition motifs: a quest in the past and future. Immunol. Rev. 224, 11–43. https://doi.org/10.1111/j.1600-065X.2008.00666.x.

DeLuca, D., Wilson, M., Warr, G.W., 1983. Lymphocyte heterogeneity in the trout, Salmo gairdneri, defined with monoclonal antibodies to IgM. Eur. J. Immunol. 13 (7), 546–551. https://doi.org/10.1002/eji.1830130706.

Dornburg, A., Wcisel, D.J., Zapfe, K., Ferraro, E., Roupe-Abrams, L., Thompson, A.W., Braasch, I., Ota, T., Yoder, J.A., 2021. Holosteans contextualize the role of the teleost genome duplication in promoting the rise of evolutionary novelties in the ray-finned fish innate immune system. Immunogenetics 73 (6), 479–497. https://doi.org/10.1007/s00251-021-01225-6.

Etayo, A., Bjørgen, H., Koppang, E.O., Hordvik, I., 2022. The teleost polymeric Ig receptor counterpart in ballan wrasse (Labrus bergylta) differs from pIgR in higher vertebrates. Vet. Immunol. Immunopathol. 249, 110440 https://doi.org/10.1016/j.vetimm.2022.110440.

Evenhuis, J., Bengtén, E., Snell, C., Quiniou, S.M., Miller, N.W., Wilson, M., 2007. Characterization of additional novel immune type receptors in channel catfish, Ictalurus punctatus. Immunogenetics 8, 661–671. https://doi.org/10.1007/s00251-007-0230-x.

Fei, C., Pemberton, J.G., Lillico, D.M.E., Zwozdesky, M.A., Stafford, J.L., 2016. Biochemical and functional insights into the integrated regulation of innate immune cell responses by teleost leukocyte immune-type receptors. Biology 5 (1), 13. https://doi.org/10.3390/biology5010013.

Fei, C., Zwozdesky, M.A., Stafford, J.L., 2020. A fish leukocyte immune-type receptor uses a novel intracytoplasmic tail networking mechanism to cross-inhibit the phagocytic response. Int. J. Mol. Sci. 21 (14), 5146. https://doi.org/10.3390/ijms21145146.

Gao, F.X., Lu, W.J., Wang, Y., Zhang, Q.Y., Zhang, Y.B., Mou, C.Y., Li, Z., Zhang, X.J., Liu, C.W., Zhou, L., Gui, J.F., 2018. Differential expression and functional diversification of diverse immunoglobulin domain-containing protein (DICP) family in three gynogenetic clones of gibel carp. Dev. Comp. Immunol. 84, 396–407. https://doi.org/10.1016/j.dci.2018.03.013.

Haire, R.N., Cannon, J.P., O'Driscoll, M.L., Ostrov, D.A., Mueller, M.G., Turner, P.M., Litman, R.T., Litman, G.W., Yoder, J.A., 2012. Genomic and functional characterization of the diverse immunoglobulin domain-containing protein (DICP) family. Genomics 99 (5), 282–291. https://doi.org/10.1016/j.ygeno.2012.02.004.

Hogan, R.J., Waldbieser, G.C., Goudie, C.A., Antao, A., Godwin, U.B., Wilson, M.R., Miller, N.W., Clem, L.W., McConnell, T.J., Wolters, W.R., Chinchar, V.G., 1999. Molecular and immunologic characterization of gynogenetic channel Catfish (*Ictalurus punctatus*). Mar. Biotechnol. 1 (4), 317–327. https://doi.org/10.1007/pl00011781.

Jones, L.O., Stafford, J.L., 2019. Imaging flow cytometry and confocal microscopy-based examination of F-actin and phosphoinositide dynamics during leukocyte immune-type receptor-mediated phagocytic events. Dev. Comp. Immunol. 92, 199–211. https://doi.org/10.1016/j.dci.2018.11.018.

Karnell, J.L., Dimasi, N., Karnell III, F.G., Fleming, R., Kuta, E., Wilson, M., Wu, H., Gao, C., Herbst, R., Ettinger, R., 2014. CD19 and CD32b differentially regulate human B cell responsiveness. J. Immunol. 192 (4), 1480–1490. https://doi.org/10.4049/jimmunol.1301361.

Kock, H., Fischer, U., 2008. A novel immunoglobulin-like transcript from rainbow trout with two Ig-like domains and two isoforms. Mol. Immunol. 45 (6), 1612–1622. https://doi.org/10.1016/j.molimm.2007.10.005.

Kortum, A.N., Rodriguez-Nunez, I., Yang, J., Shim, J., Runft, D., O'Driscoll, M.L., Haire, R.N., Cannon, J.P., Turner, P.M., Litman, R.T., Kim, C.H., Neely, M.N., Litman, G.W., Yoder, J.A., 2014. Differential expression and ligand binding indicate alternative functions for zebrafish polymeric immunoglobulin receptor (pIgR) and a family of pIgR-like (PIGRL) proteins. Immunogenetics 66 (4), 267–279. https://doi.org/10.1007/s00251-014-0759-4.

Kuroki, K., Furukawa, A., Maenaka, K., 2012. Molecular recognition of paired receptors in the immune system. Front. Microbiol. 3, 429. https://doi.org/10.3389/fmicb.2012.00429.

Lanier, L.L., 2009. DAP10- and DAP12-associated receptors in innate immunity. Immunol. Rev. 227 (1), 150–160. https://doi.org/10.1111/j.1600-065X.2008.00720.x.

Levi-Schaffer, F., Mandelboim, O., 2018. Inhibitory and coactivating receptors recognising the same ligand: immune homeostasis exploited by pathogens and tumours. Trends Immunol. 39 (2), 112–122. https://doi.org/10.1016/j.it.2017.10.001.

Lillico, D., Pemberton, J.G., Stafford, J.L., 2018. Selective regulation of cytoskeletal dynamics and filopodia formation by teleost leukocyte immune-type receptors differentially contributes to target capture during the phagocytic process. Front. Immunol. 9, 1144. https://doi.org/10.3389/fimmu.2018.01144.

Lillico, D.M., Zwozdesky, M.A., Pemberton, J.G., Deutscher, J.M., Jones, L.O., Chang, J. P., Stafford, J.L., 2015. Teleost leukocyte immune-type receptors activate distinct phagocytic modes for target acquisition and engulfment. J. Leukoc. Biol. 2, 235–248. https://doi.org/10.1189/jlb.2A0215-039RR.

Lillico, D.M.E., Pemberton, J.G., Niemand, R., Stafford, J.L., 2020. Selective recruitment of Nck and Syk contribute to distinct leukocyte immune-type receptor-initiated target interactions. Cell Signal 66, 109443. https://doi.org/10.1016/j.cellsig.2019.109443.

Martinet, L., Smyth, M.J., 2015. Balancing natural killer cell activation through paired receptors. Nat. Rev. Immunol. 15 (4), 243–254. https://doi.org/10.1038/nri3799.

Mewes, J., Verheijen, K., Montgomery, B.C., Stafford, J.L., 2009. Stimulatory catfish leukocyte immune-type receptors (IpLITRs) demonstrate a unique ability to associate with adaptor signaling proteins and participate in the formation of homo- and heterodimers. Mol. Immunol. 47, 318–331. https://doi.org/10.1016/j.molimm.2009.09.014.

Miller, N., Wilson, M., Bengtén, E., Stuge, T., Warr, G., Clem, W., 1998. Functional and molecular characterization of teleost leukocytes. Immunol. Rev. 166, 187–197. https://doi.org/10.1111/j.1600-065x.1998.tb01263.x.

Miller, N.W., Bly, J.E., van Ginkel, F., Ellsaesser, C.F., Clem, L.W., 1987. Phylogeny of lymphocyte heterogeneity: identification and separation of functionally distinct subpopulations of channel catfish lymphocytes with monoclonal antibodies. Dev. Comp. Immunol. 11, 739–747.

Miller, N.W., Rycyzyn, M.A., Wilson, M.R., Warr, G.W., Naftel, J.P., Clem, L.W., 1994. Development and characterization of channel catfish long term B cell lines. J. Immunol. 152 (5), 2180–2189.

Miller, N.W., Chinchar, V.G., Clem, L.W., 1994. Development of leukocyte cell lines from the channel catfish (*Ictalurus punctatus*). J. Tissue Cult. Methods 16, 117–123.

Montgomery, B.C., Mewes, J., Davidson, C., Burshtyn, D.N., Stafford, J.L., 2009. Cell surface expression of channel catfish leukocyte immune-type receptors (IpLITRs) and recruitment of both Src homology 2 domain-containing protein tyrosine phosphatases (SHP)-1 and SHP-2. Dev. Comp. Immunol. 33, 570–582. https://doi.org/10.1016/j.dci.2008.10.006.

Montgomery, B.C., Cortes, H.D., Burshtyn, D.N., Stafford, J.L., 2012. Channel catfish leukocyte immune-type receptor mediated inhibition of cellular cytotoxicity is facilitated by SHP-1-dependent and -independent mechanisms. Dev. Comp. Immunol. 37 (1), 151–163. https://doi.org/10.1016/j.dci.2011.09.005.

Moretta, A., Pantaleo, G., Lopez-Botet, M., Moretta, L., 1985. Selection and characterization of monoclonal antibodies to the idiotype-like structure of an interleukin-2–producing human leukemia t-cell line. Int. J. Cancer 36, 253–259. https://doi.org/10.1002/ijc.2910360219.

Moulana, M., Evenhuis, J., Albertino, M., Godwin, U., Kountikov, E.I., Stuge, T.B., Wilson, M., Bengtén, E., Miller, N.W., McConnell, T.J., 2008. Characterization of anti-channel catfish MHC class IIbeta monoclonal antibodies. Vet. Immunol. Immunopathol. 126 (1–2), 120–130. https://doi.org/10.1016/j.vetimm.2008.06.012.

Østergaard, A.E., Martin, S.A., Wang, T., Stet, R.J., Secombes, C.J., 2009. Rainbow trout (*Oncorhynchus mykiss*) possess multiple novel immunoglobulin-like transcripts containing either an ITAM or ITIMs. Dev. Comp. Immunol. 33 (4), 525–532. https://doi.org/10.1016/j.dci.2008.10.002.

Østergaard, A.E., Lubieniecki, K.P., Martin, S.A., Stet, R.J., Davidson, W.S., Secombes, C. J., 2010. Genomic organisation analysis of novel immunoglobulin-like transcripts in Atlantic salmon (*Salmo salar*) reveals a tightly clustered and multigene family. BMC Genom. 11, 697. https://doi.org/10.1186/1471-2164-11-697.

Ribeiro, C.M., Bird, S., Raes, G., Ghassabeh, G.H., Schijns, V.E., Pontes, M.J., Savelkoul, H.F., Wiegertjes, G.F., 2011. A novel soluble immune-type receptor (SITR) in teleost fish: carp SITR is involved in the nitric oxide-mediated response to a protozoan parasite. PLoS One 6 (1), e15986. https://doi.org/10.1371/journal.pone.0015986.

Rodriguez-Nunez, I., Wcisel, D.J., Litman, R.T., Litman, G.W., Yoder, J.A., 2016. The identification of additional zebrafish DICP genes reveals haplotype variation and linkage to MHC class I genes. Immunogenetics 68 (4), 295–312. https://doi.org/10.1007/s00251-016-0901-6.

Rodríguez-Nunez, I., Wcisel, D.J., Litman, G.W., Yoder, J.A., 2014. Multigene families of immunoglobulin domain-containing innate immune receptors in zebrafish: deciphering the differences. Dev. Comp. Immunol. 46 (1), 24–34. https://doi.org/10.1016/j.dci.2014.02.004.

Schwarz, F., Landig, C.S., Siddiqui, S., Secundino, I., Olson, J., Varki, N., Nizet, V., Varki, A., 2017. Paired Siglec receptors generate opposite inflammatory responses to a human-specific pathogen. EMBO J. 36 (6), 751–760. https://doi.org/10.15252/embj.201695581.

Shen, L., Stuge, T.B., Zhou, H., Khayat, M., Barker, K.S., Quiniou, S.M., Wilson, M., Bengtén, E., Chinchar, V.G., Clem, L.W., Miller, N.W., 2002. Channel catfish cytotoxic cells: a minireview. Dev. Comp. Immunol. 26, 141–149. https://doi.org/10.1016/s0145-305x(01)00056-8.

Shen, L., Stuge, T.B., Evenhuis, J.P., Bengtén, E., Wilson, M., Chinchar, V.G., Clem, L.W., Miller, N.W., 2003. Channel catfish NK-like cells are armed with IgM via a putative FcμR. Dev. Comp. Immunol 699–714. https://doi.org/10.1016/s0145-305x(03)00042-9.

Shen, L., Stuge, T.B., Bengtén, E., Wilson, M., Chinchar, V.G., Naftel, J.P., Bernanke, J. M., Clem, L.W., Miller, N.W., 2004. Identification and characterization of clonal NK-like cells from channel catfish (Ictalurus punctatus). Dev. Comp. Immunol. 28, 139–152. https://doi.org/10.1016/s0145-305x(03)00119-8.

Stafford, J.L., Bengtén, E., Du Pasquier, L., McIntosh, R.D., Quiniou, S.M., Clem, L.W., Miller, N.W., Wilson, M., 2006. A novel family of diversified immunoregulatory receptors in teleosts is homologous to both mammalian fc receptors and molecules encoded within the leukocyte receptor complex. Immunogenetics 758–773. https://doi.org/10.1007/s00251-006-0134-1.

Stafford, J.L., Bengtén, E., Du Pasquier, L., Miller, N.W., Wilson, M., 2007. Channel catfish leukocyte immune-type receptors (LITRs) contain a putative MHC class I binding site. Immunogenetics 59, 77–91. https://doi.org/10.1007/s00251-006-0169-3.

Stet, R.J., Hermsen, T., Westphal, A.H., Jukes, J., Engelsma, M., Lidy Verburg-van Kemenade, B.M., Dortmans, J., Aveiro, J., Savelkoul, H.F., 2005. Novel immunoglobulin-like transcripts in teleost fish encode polymorphic receptors with cytoplasmic ITAM or ITIM and a new structural Ig domain similar to the natural cytotoxicity receptor NKp44. Immunogenetics 57 (1–2), 77–89. https://doi.org/10.1007/s00251-005-0771-9.

Strong, S.J., Mueller, M.G., Litman, R.T., Hawke, N.A., Haire, R.N., Miracle, A.L., et al., 1999. A novel multigene family encodes diversified variable regions. Proc. Natl. Acad. Sci. U. S. A 96 (26), 15080–15085. https://doi.org/10.1073/pnas.96.26.15080.

Stuge, T.B., Yoshida, S.H., Chinchar, V.G., Miller, N.W., Clem, L.W., 1997. Cytotoxic activity generated from channel catfish peripheral blood leukocytes in mixed leukocyte cultures. Cell Immunol. 177 (2), 154–161. https://doi.org/10.1006/cimm.1997.1106.

Stuge, T.B., Wilson, M.R., Zhou, H., Barker, K.S., Bengtén, E., Chinchar, G., Miller, N.W., Clem, L.W., 2000. Development and analysis of various clonal alloantigen-dependent cytotoxic cell lines from channel catfish. J. Immunol. 164, 2971–2977. https://doi.org/10.4049/jimmunol.164.6.2971.

Taylor, E.B., Moulana, M., Stuge, T.B., Quiniou, S.M.A., Bengten, E., Wilson, M., 2016. A leukocyte immune-type receptor subset is a marker of antiviral cytotoxic cells in channel catfish, Ictalurus punctatus. J. Immunol. 196, 2677–2689. https://doi.org/10.4049/jimmunol.1502166.

Taylor, E.B., Chinchar, V.G., Quiniou, S.M.A., Wilson, M., Bengtén, E., 2020. Cloning and characterization of antiviral cytotoxic T lymphocytes in channel catfish, Ictalurus punctatus. Virology 540, 184–194. https://doi.org/10.1016/j.virol.2019.11.014.

Tolnay, M., 2022. Lymphocytes sense antibodies through human FCRL proteins: emerging roles in mucosal immunity. J. Leukoc. Biol. 111 (2), 477–487. https://doi.org/10.1002/JLB.4RU0221-102RR.

Vallejo, A.N., Ellsaesser, C.F., Miller, N.W., Clem, L.W., 1991. Spontaneous development of functionally active long-term monocyte-like cell lines from channel catfish. Vitr. Cell. Dev. Biol. 27A, 279–286.

van Ginkel, F.W., Miller, N.W., Lobb, C.J., Clem, L.W., 1992. Characterization of anti-hapten antibodies generated in vitro by channel catfish peripheral blood lymphocytes. Dev. Comp. Immunol. 16, 139–151. https://doi.org/10.1016/0145-305x(92)90014-4.

Vély, F., Vivier, E., 1997. Conservation of structural features reveals the existence of a large family of inhibitory cell surface receptors and noninhibitory/activatory counterparts. J. Immunol. 8, 1994–2000.

Wan, F., Hu, C.B., Ma, J.X., Gao, K., Xiang, L.X., Shao, J.Z., 2017. Characterization of γδ T cells from zebrafish provides insights into their important role in adaptive humoral immunity. Front. Immunol. 7, 675. https://doi.org/10.3389/fimmu.2016.00675.

Wang, J., Belosevic, M., Stafford, J.L., 2020. Identification of goldfish (*Carassius auratus L.*) leukocyte immune-type receptors shows alternative splicing as a potential mechanism for receptor diversification. Mol. Immunol. 125, 83–94. https://doi.org/10.1016/j.molimm.2020.06.024.

Wang, J., Belosevic, M., Stafford, J.L., 2021. Identification of distinct LRC- and Fc receptor complex-like chromosomal regions in fish supports that teleost leukocyte immune-type receptors are distant relatives of mammalian Fc receptor-like molecules. Immunogenetics 73 (1), 93–109. https://doi.org/10.1007/s00251-020-01193-3.

Wcisel, D.J., Dornburg, A., McConnell, S.C., Hernandez, K.M., Andrade, J., de Jong, J., Litman, G.W., Yoder, J.A. , 2022. A highly diverse set of novel immunoglobulin-like transcript (NILT) genes in zebrafish indicates a wide range of functions with complex relationships to mammalian receptors. Immunogenetics. 10.1007/s00251–022-01270–9. Advance online publication. ⟨https://doi.org/10.1007/s00251–022-01270–9⟩.

Wei, S., Zhou, J.M., Chen, X., Shah, R.N., Liu, J., Orcutt, T.M., Traver, D., Djeu, J.Y., Litman, G.W., Yoder, J.A., 2007. The zebrafish activating immune receptor Nitr9 signals via Dap12. Immunogenetics 59 (10), 813–821. https://doi.org/10.1007/s00251-007-0250-6.

Wilson, M., Bengtén, E., Miller, N.W., Clem, L.W., Du Pasquier, L., Warr, G.W., 1997. A novel chimeric Ig heavy chain from a teleost fish shares similarities to IgD. Proc. Natl. Acad. Sci. USA 94 (9), 4593–4597. https://doi.org/10.1073/pnas.94.9.4593.

Wilson, M.R., Zhou, H., Bengten, E., Clem, L.W., Stuge, T.B., Warr, G.W., Miller, N.W., 1998. T cell receptors in channel catfish: structure and expression of TCR alpha and beta genes. Mol. Immunol. 35, 545–557. https://doi.org/10.1016/s0161-5890(98)00037-6.

Wu, Y., Wu, W., Wong, W.M., Ward, E., Thrasher, A.J., Goldblatt, D., Osman, M., Digard, P., Canaday, D.H., Gustafsson, K., 2009. Human gamma delta T cells: a lymphoid lineage cell capable of professional phagocytosis. J. Immunol. 183 (9), 5622–5629. https://doi.org/10.4049/jimmunol.0901772.

Yamada, E., McVicar, D.W., 2008. Paired receptor systems of the innate immune system. Curr. Protoc. Immunol. Chapter 1, Append. 1X. https://doi.org/10.1002/0471142735.ima01xs81.

Yoder, J.A., Mueller, M.G., Wei, S., Corliss, B.C., Prather, D.M., Willis, T., et al., 2001. Immune-type receptor genes in zebrafish share genetic and functional properties with genes encoded by mammalian leukocyte receptor cluster. Proc. Natl. Acad. Sci. U. S. A. 98 (12), 6771–6776. https://doi.org/10.1073/pnas.121101598.

Yoder, J.A., Litman, R.T., Mueller, M.G., Desai, S., Dobrinski, K.P., Montgomery, J.S., Buzzeo, M.P., Ota, T., Amemiya, C.T., Trede, N.S., Wei, S., Djeu, J.Y., Humphray, S., Jekosch, K., Hernandez Prada, J.A., Ostrov, D.A., Litman, G.W., 2004. Resolution of the novel immune-type receptor gene cluster in zebrafish. Proc. Natl. Acad. Sci. USA 101 (44), 15706–15711. https://doi.org/10.1073/pnas.0405242101.

Zwozdesky, M.A., Fei, C., Lillico, D.M.E., Stafford, J.L., 2017. Imaging flow cytometry and GST pulldown assays provide new insights into channel catfish leukocyte immune-type receptor-mediated phagocytic pathways. Dev. Comp. Immunol. 67, 126–138. https://doi.org/10.1016/j.dci.2016.10.011.